Scd1 diffuses end to end along the cytoplasm to facilitate Cdc42 activation and bipolar growth

Marcus A Harrell*[1], Olivia Chinsen[1], Maitreyi Das[1§]

[1] Biology Department, Boston College, Chestnut Hill, MA, 02467

[§] **Corresponding author:** Maitreyi.Das@bc.edu

Running title: Scd1 diffusion drives bipolar growth

ABSTRACT

The GTPase Cdc42 is highly conserved and a major regulator of polarized growth in most eukaryotes. In the fission yeast *S. pombe*, Cdc42 activity oscillates at the ends for bipolar growth. Both ends are not simultaneously active, and the active end must lose Cdc42 activation for the other end to gain Cdc42 activity. This suggests that some component of Cdc42 activation must diffuse from one end to the next to activate Cdc42 via the oscillatory pattern. We hypothesize that ends compete for limited Scd1 that diffuses through the cytoplasm to promote bipolar growth. We tested this by quantifying the impact of increased Scd1 mass on cell morphology and protein dynamics. We find that increasing mass on Scd1 leads to dampened Cdc42 activation and more monopolar cells due to slowed Scd1 localization. Our data show that while the mass of Scd1 does play a role in its diffusion dynamics, its intrinsic properties and Pak1 kinase play a more important role. Our findings highlight the role of a previously unknown factor, cytoplasmic diffusion of activators, in regulating cell polarity.

SUMMARY

Scd1 (GEF) activates Cdc42 for polarized cell growth. We show that Scd1 undergoes cytoplasmic diffusion between the two cell ends. This diffusion is not random and likely depends on intrinsic properties of the Scd1 protein.

Keywords: Cdc42, oscillations, Scd1, diffusion, Pak1 kinase, cell polarity

29 **INTRODUCTION**

30 The Rho Family GTPase Cdc42 is a major regulator of polarized growth across most
31 eukaryotes (Johnson, 1999; Miller and Johnson, 1994). Cdc42 is a molecular switch that is
32 active when GTP bound, and subsequently inactivated when GTP is hydrolyzed to GDP
33 (Johnson, 1999). Active Cdc42 promotes F-actin polymerization and membrane trafficking for
34 cell growth. Thus, Cdc42 activity must be precisely coordinated among multiple sites of growth
35 for proper cell polarity and function (Das and Verde, 2013; Nobes and Hall, 1999; Stengel and
36 Zheng, 2011). GTPases are activated by GEFs (Guanine nucleotide exchange factors) and
37 inactivated by GAPs (GTPase activating proteins) (Hall, 1990). GEFs activate Cdc42 by
38 exchanging GDP for GTP, while GAPs complete a catalytic triad to promote hydrolysis of GTP
39 into GDP (Scheffzek and Ahmadian, 2005; Zhang et al., 1999).

40 The fission yeast *S. pombe* has a streamlined proteome when compared to more
41 complex model systems. For example, Cdc42 has around 20 GEFs and GAPs in mammalian
42 cells (Rossman et al., 2005). But, in *S. pombe*, there are only two Cdc42 GEFs, Scd1 and Gef1,
43 and three Cdc42 GAPs (Coll et al., 2003; Murray and Johnson, 2001). These streamlined
44 signaling pathways make *S. pombe* an excellent model to investigate Cdc42 regulation. *S.*
45 *pombe* has 3 major players for Cdc42 activation and growth, Gef1, Scd1, and the scaffold Scd2
46 (Chang et al., 1999; Chang et al., 1994; Sawin and Nurse, 1998; Wheatley and Rittinger, 2005).
47 Upstream Ras signaling promotes the initial activation of Cdc42 (Chang et al., 1994). When
48 active, GTP-bound Cdc42 recruits Scd2 (Bem1p) to tether Scd1 (Cdc24p) to the membrane and
49 activate more Cdc42 (Butty et al., 2002; Rapali et al., 2017; Wheatley and Rittinger, 2005). This
50 results in a positive-feedback loop wherein Cdc42 activation continuously activates more Cdc42
51 thus becoming a self-amplifying system (Butty, 2002; Das and Verde, 2013; Kozubowski et al.,
52 2008).

53 During interphase, Cdc42 activity oscillates and Cdc42 activation continually rises and
54 falls at the two growing ends (Das et al., 2012). Further, it has been shown that Cdc42
55 oscillations are anti-correlated, such that as one end has high Cdc42 activity, the other end has
56 low Cdc42 activation and the higher end must begin to lose Cdc42 activity for the opposite end
57 to increase Cdc42 activation (Das et al., 2012). This spatiotemporal patterning suggests that the
58 two ends are interconnected such that a factor is alternately recruited to the growing cell ends
59 for oscillatory activation of Cdc42.

60 The identity of this factor or how it travels from one end to the other is unknown but
61 Cdc42 GEFs are a likely candidate. Previous work has shown Gef1 and Scd1 play distinct roles
62 in cytokinesis and Gef1 is a secondary GEF for Cdc42 activation and initiates growth at new
63 sites but is not the major GEF needed for polarized growth (Hercyk et al., 2019; Wei et al.,
64 2016). Indeed, *gef1*Δ mutants are mostly monopolar, but still polarized whereas *scd1*Δ mutants
65 are not polarized, and show spherical morphology (Hercyk et al., 2019). This suggests that
66 Scd1 is the primary GEF for cell polarity. Cdc42 oscillatory dynamics occur due to time-delayed
67 negative feedback where the Pak1 kinase prevents Scd1 recruitment to the cell membrane (Das
68 et al., 2012). We have recently shown Scd1 returns to each cell end after inhibition by Pak1
69 kinase in an endocytosis-dependent manner. Pak1 kinase at each end is removed during
70 endocytosis and this allows the return of Scd1 for the next cycle of Cdc42 activation at that end
71 (Harrell et al., 2024). We asked if the population of Scd1 within the cell sequentially moves from
72 one end to the other for oscillatory Cdc42 activation.

73 To this end, we used *in vivo* experiments in *S. pombe* to test if Scd1 travels from one
74 end to the other to promote bipolar growth. We find that in fission yeast, Scd1 is mostly
75 cytoplasmic and its localization to the ends is not dependent on actin-mediated delivery. Our
76 data shows that Scd1 diffuses between the two halves of the cell. Furthermore, Pak1 kinase
77 promotes faster diffusion of Scd1 within the cell. We show that Scd2 also localizes via

78 cytoplasmic diffusion, yet Scd1 molecules have a faster turnover between the two halves of the
79 cell and their growing ends when compared to Scd2 despite Scd2 being a smaller and more
80 abundant protein. Our data also show that simply increasing the mass of Scd1 does not linearly
81 decrease its diffusion dynamics even though it impacts its ability to promote bipolarity. Together
82 our findings here show that Scd1 diffuses from one end of the cell to the other to promote
83 oscillatory behavior but this does not occur via simple random diffusion and likely depends on
84 the properties and regulation of Scd1.

85 **RESULTS & DISCUSSION**

86 **Scd1 is highly cytoplasmic and diffuses between cell ends**

87 It is unknown how Scd1 is delivered to the cell ends for activation of Cdc42. We asked if
88 Scd1 localizes to the cell ends via membrane trafficking. We previously reported that Scd1
89 localization is diminished at cell ends upon depolymerization of all F-actin during LatA treatment
90 (Hercyk et al., 2019). Thus, we asked if Scd1 was delivered via actin cables. We used *for3*Δ
91 mutants, which cannot polymerize linear actin cables for actin-mediated delivery during
92 interphase (Feierbach and Chang, 2001; Martin and Chang, 2006; Nakano et al., 2002). We
93 compared Scd1-mNG localization in *for3*$^{+}$ cells and *for3*Δ mutants and found that Scd1
94 localization is not decreased by the lack of actin-mediated delivery (Fig. 1A, B). Together, these
95 data suggest that Scd1 is not localized by actin-mediated membrane trafficking. Furthermore,
96 bipolar *for3*Δ mutants show increased Scd1 localization and anticorrelated Cdc42 oscillations
97 thus suggesting that actin does not facilitate delivery of Scd1.

98 Many yeast proteins localize in the cytoplasm as part of their function (Matsuyama et al.,
99 2006). Fluorescent microscopy of Scd1 shows high cytoplasmic fluorescence intensity relative
100 to the cell ends (Fig. 1A). We quantified the distribution of Scd1-mNG intensity throughout the
101 cell and find that Scd1 localization within the cytoplasm is high even when compared to the
102 more intense cell end (Fig. 1C). To quantify this metric, we averaged the intensity of the
103 cytoplasm and compared the cytoplasmic intensity to the two cell ends and found that the
104 cytoplasmic intensity of Scd1-mNG is about 50% of the total Scd1-mNG localized at the cell
105 ends (Fig. 1D). This suggests that there is a high ratio of Scd1-mNG that is localized in the
106 cytoplasm of the cell despite the low abundance of Scd1.

107 It has been established that the diffusion of solutes and macromolecules is important for
108 several cellular processes (Verkman, 2002). Due to high levels of Scd1-mNG in the cytoplasm
109 and Scd1-mNG localization occurring independent of membrane trafficking, we hypothesized

110 that Scd1-mNG may localize to cell ends via diffusion. To test this, we used fluorescence loss in
111 photobleaching (FLIP) (Cole et al., 1996; Shcheprova et al., 2008; White and Stelzer, 1999).
112 FLIP is a photomanipulation technique that measures the rate of protein exchange between two
113 regions of interest within a cell by repeatedly bleaching one area of the cell while measuring the
114 rate of fluorescence loss at a second region of interest within the cell. If fluorescence is lost at
115 the second region, this suggests that the two regions of interest exchange proteins (White and
116 Stelzer, 1999). Further, the rate of this loss can be used to approximate the rate of protein
117 exchange between these regions (Fig. 1E, top). If there is no exchange between the two regions
118 of interest, no loss in fluorescence will be observable at the second site (Fig. 1E, bottom).
119 We used FLIP to test if Scd1 is exchanged between the two ends of bipolar cells or if
120 each end has a distinct pool of Scd1. We bleached within the cytoplasm to ensure consistent
121 photobleaching for each experiment and fluorescence loss was observed at the cell end of the
122 opposite half of the cell from where cytoplasmic beaching occurs (Fig. 1F). We performed FLIP
123 on Scd1-mNG cells and found that the two halves of the cell do exchange Scd1-mNG, as one
124 half's cytoplasm is bleached, the growing end of the opposite half steadily loses fluorescence
125 above the rate of photobleaching (Fig. 1F and Fig. S2A). Notably, the low signal-to-noise ratio of
126 Scd1-mNG combined with photobleaching correction, results in a plateau of intensity when all
127 fluorescence has been lost (Fig. 1F, G). We found that the average time to lose 50%
128 fluorescence intensity from the opposing cell end was around 75 seconds (Fig. 1H). These
129 findings suggest that Scd1 is exchanged between the two halves of the cell and that Scd1 may
130 localize via diffusion.
131

132 **Increasing mass on Scd1 dampens Cdc42 activation and increases monopolarity**

133 We next asked if Scd1 dynamics can be dampened by increasing the mass on the
134 protein. Because Scd1 is the major activator of Cdc42, dampened Scd1 dynamics likely disrupts
135 proper Cdc42 activity. To test this, we observed CRIB-mCherry dynamics, which specifically
136 localize to the active form of Cdc42, in Scd1-mNG and Scd1-3xGFP strains (Fig. 2A). Scd1 is a
137 99.1kDa protein and each fluorophore adds roughly 26.6 kDa of mass. We tested Cdc42
138 activation dynamics in -mNG (+26.6 kDa) and -3xGFP strains (+79.8 kDa). Indeed, we find that
139 CRIB-mCherry oscillates between the two ends as expected in Scd1-mNG cells however CRIB-
140 mCherry dynamics are notably more monopolar in Scd1-3xGFP cells (Fig. 2A, B). To quantify
141 this difference, we measured how much CRIB-mCherry fluctuated between each time point at
142 the weaker cell ends and find that Cdc42 activation is less dynamic when Scd1 is too massive
143 as seen with CRIB-mCherry in Scd1-3xGFP expressing cells (Fig. 2C).

144 To test the impact of adding additional mass to Scd1 on cell polarity, we stained cells
145 with calcofluor white to quantify the percentage of monopolar cells in cultures of cells with
146 fluorescently tagged Scd1. In addition to -mNG and -3xGFP, we also tested strains with -
147 tdTomato and -2xGFP (+54.2 kDa). We find there is an increased percentage of monopolar
148 cells as more mass is added to Scd1 suggesting that increased Scd1 mass dampens bipolar
149 Cdc4 activation and results in monopolar cells (Fig. 2D and Fig. S2A). In cells with increased
150 Scd1 mass a smaller but consistent fraction of the cells are bipolar, suggesting that it is rare but
151 still possible for Scd1 to accumulate at the opposite end. But under these conditions, this
152 evolutionary important system of bipolar growth no longer consistently functions within the
153 population (Fig. 2D).

154

155

156

157 **Increasing the mass on Scd1 does not proportionally decrease its diffusion dynamics**

158 Since Scd1 diffuses from one end of the cell to the other and increasing the mass of
159 Scd1 leads to increased monopolarity and altered Cdc42 activation patterns, we asked if Scd1
160 is distributed between ends via random diffusion in the cytoplasm. If this is true, the decrease in
161 Scd1 diffusion should be proportionally inverse to the increase in mass of this protein. We
162 aimed to test if Scd1 diffusion and localization to cell ends is slowed by adding more mass to
163 Scd1. We used FLIP to test if Scd1 diffusion was slower in populations that have more mass
164 added to Scd1 (Fig. 3A and Fig. S3A). We tested the rate of Scd1 loss in -mNG (+26.6 kDa), -
165 2xGFP (+53.2 kDa), and -3xGFP strains (+79.8 kDa) (Fig. 3B and Fig. S3A). We find that there
166 is a significant dampening of the rate of Scd1 loss in -2xGFP and -3xGFP strains when
167 compared to -mNG (Fig. 3C and Fig. S3A). While the half-life of Scd1-mNG fluorescence at the
168 cell end is still lost around 70 seconds, Scd1-2xGFP and Scd1-3xGFP cells show a half-life of
169 around 100 seconds. This suggests that additional mass does hinder Scd1 mobility and
170 dampens its dynamics. However, we did not see any change in the diffusion dynamics between
171 Scd1-2xGFP and Scd1-3xGFP. This indicates that the while a change in Scd1 mass alters its
172 diffusion dynamics, other factors also regulate its diffusion dynamics.

173 Next, we tested if Scd1 recruitment at the cell ends is perturbed by additional mass. To
174 this end, we used fluorescence recovery after photobleaching (FRAP) for these investigations
175 (Axelrod et al., 1976; Jacobson et al., 1976; Poo and Cone, 1974). We bleached half of one cell
176 end to standardize the amount of bleaching and observe if the arrival of unbleached, new
177 protein occurred via lateral membrane diffusion or cytoplasmic diffusion (Fig. 3C). We observe
178 that Scd1 recovery at the photobleached region occurs without diminishing the intensity of the
179 other half of the same cell end which suggests that recovery occurs via the arrival of protein
180 from the cytoplasm and not due to the diffusion of the protein from one side of the end to the
181 bleached side (Fig. S3B, and Fig. S3C). Indeed, we found that Scd1 fluorescence recovery is

182 significantly slower in -2xGFP and -3xGFP strains when compared to Scd1-mNG (Fig. 3D, E).
183 However, similar to our FLIP data, we did not see any difference in the FRAP recovery of Scd1-
184 2xGFP and Scd1-3xGFP. This further suggests that Scd1 dynamics at the cell ends are only
185 partially dependent on its mass.

186 **Pak1 kinase facilitates Scd1 diffusion dynamics within the cell.**

187 In budding yeast, Cdc42 activates the PAK Kinase, Pak1 (Cla4), to phosphorylate and inhibit
188 Scd1 (Cdc24) localization at cell ends via negative feedback (Gulli et al., 2000; Howell et al.,
189 2012; Kuo et al., 2014; Rapali et al., 2017; Wu et al., 2015; Wu and Lew, 2013). In fission yeast
190 *pak1-ts* hypomorphic mutants, high amounts of Scd1 and active Cdc42 accumulate at only one
191 end causing the characteristic monopolar and wide phenotype (Das et al., 2012; Verde et al.,
192 1998). We asked if Pak1 kinase also regulated Scd1 diffusion within the cytoplasm. To this end,
193 we investigated the rate of Scd1-mNG recruitment and diffusion using FRAP and FLIP in a
194 *pak1-ts* mutant background. We used FRAP to measure Scd1-mNG recruitment to cell ends in
195 *pak1-ts* mutants and found there is no significant difference between *pak1*$^{+}$ cells and *pak1-ts*
196 mutants (Fig. 4A, B, C). This suggests that the lack of Pak1 kinase on Scd1 does not
197 significantly impact Scd1-mNG recruitment to cell ends (Fig. 4A, B, C). Next, we used FLIP and
198 measured fluorescence loss at the cell ends to quantify if the lack of Pak1 kinase impacted
199 Scd1 diffusion. We find that Scd1-mNG intensity loss is significantly slower in *pak1-ts* mutants
200 when compared to *pak1*$^{+}$ cells (Fig. 4D). The half-life of fluorescence loss of Scd1-mNG in
201 *pak1*$^{+}$ cells is 74 seconds while that in *pak1-ts* mutants is 140 seconds (Fig. 4E). These data
202 suggest that in the absence of Pak1 kinase activity, Scd1-mNG diffusion is significantly delayed
203 and even slower than Scd1-2xGFP and Scd1-3xGFP. The mechanism of how Pak1-dependent
204 phosphorylation of Scd1 diffusion will be investigated further in future studies.

205

206 **The scaffold Scd2 shows slower diffusion dynamics compared to Scd1**

207 We asked if like Scd1, its scaffold Scd2 also diffused from one end of the cell to the
208 other with similar dynamics? It is possible that the dynamics of Scd2, the Scd1 scaffold, dictates
209 the rate of Scd1 diffusion to the sites of growth. To test this possibility, we compared the rates of
210 diffusion between Scd1-mNG and Scd2-GFP. We began by comparing the distribution of Scd1-
211 mNG within the cell to Scd2-GFP (Fig. 5A, B). We again see that Scd1-mNG has roughly 50%
212 of its intensity in the cytoplasm when compared to the cell ends. By contrast, Scd2-GFP only
213 shows about 25% of its intensity in the cytoplasm relative to the Scd2 intensity at the cell ends
214 (Fig. 5A, B, C). Moreover. While we see a consistent dip in Scd1 levels in the cytoplasm right
215 next to the end with increased levels, we do not such a dip for Scd2 near the ends (Fig. 5B, red
216 arrow).

217 Next, we performed FLIP on Scd1-mNG cells and Scd2-GFP cells to compare their rates
218 of exchange between the two halves of the cell (Fig. 5D). We find that like Scd1-mNG, Scd2-
219 GFP is also exchanged between the cytoplasm and cell ends. However, Scd1-mNG intensity is
220 rapidly lost from the cell end whereas Scd2-GFP loss is slower (Fig. 5D, E). The average half-
221 life of fluorescence intensity loss for Scd1-mNG is around 70 seconds on average whereas the
222 half-life of Scd2 loss is over 200 seconds (Fig. 5E, F). Together, these data suggest that while
223 Scd1 diffuses from one cell end to the other for bipolar Cdc42 activation, Scd2 diffusion is much
224 slower and thus likely not a factor in Cdc42 oscillatory dynamics. Indeed the fluorescence decay
225 of Scd2-GFP the opposite end is even slower than that Scd1-2xGFP and -3xGFP (Fig.5H).
226 Thus, Scd1 (99 kDa) has a higher ratio of cytoplasmic localization and is exchanged rapidly
227 between growing ends despite Scd2 (60 kDa) being the smaller and more abundant protein.
228 This further suggests mass is not the only factor that impacts diffusion and the intrinsic
229 properties of Scd1 facilitate its rapid diffusion.

230

231 **Conclusions**

232 We previously found that Pak1 removal via endocytosis is vital for Scd1 localization and
233 allows for the repeated cycle of Cdc42 activation at a cell end (Harrell et al., 2024). Here we
234 show that Scd1 localizes to the growing cell ends via diffusion between those ends. Thus, Pak1
235 phosphorylation must facilitate adequate Scd1 turnover at cell ends such that there is enough
236 cytoplasmic Scd1 molecules to diffuse to the other end to drive Cdc42 activation between the
237 different sites of growth. Thus, we find yet another layer of self-regulation in this polarity system
238 where Scd1 diffusion within the cytoplasm activates Cdc42 and promotes bipolar growth.

239 FLIP analysis of Scd1-3xGFP shows that when the half-life is slowed to around 100 seconds or
240 more, most cells in the population are monopolar. This suggests Scd2 is exchanged less rapidly
241 while Scd1, with a half-life of 70 seconds, must be rapidly exchanged to promote proper
242 competition and bipolar growth. The finding that Scd2 diffusion is slower than the diffusion of
243 Scd1 suggests that this diffusion is not random and that the intrinsic properties of the proteins
244 impact their diffusion rates. Scd1 has a higher amount of intrinsically disordered regions when
245 compared to Scd2. While the functional significance of IDRs remains to be fully understood,
246 speculatively, these regions may have roles in facilitating Scd1 diffusion, possibly by making the
247 protein more soluble when diffusing. IDRs or other intrinsic properties of Scd1 may explain why
248 simply increasing the mass beyond 54.2kDa (-2xGFP and -3xGFP) alone does not further
249 dampen Scd1 dynamics.

250 There is a consistent drop in cytoplasmic Scd1 intensity near the active growing end.
251 More investigation is needed to test the significance of this pattern. It is possible that this is a
252 region of active recruitment and turnover, so most Scd1 molecules that are within this region are
253 rapidly recruited to the membrane of the growing cell end. Scd1 would need to be beyond a
254 certain threshold of an active end to have a chance of diffusing to the opposite cell end. This

threshold may be easier to overcome when an end is saturated and reaches its carrying capacity such that it can no longer accumulate more Scd1.

Scd1 diffusion appears to slow down in mutants of the *pak1* kinase. In Pak1 kinase mutants Scd1 is not removed from the cell ends via negative feedback (Das et al., 2012). In these cells Scd1 accumulates at only one cell end and the cells are monopolar. These mutants do show cytoplasmic Scd1 with similar recruitment rates at the growing cell end similar to that of *pak1*$^{+}$ cells. However, they display slower diffusion rates suggesting that Pak1 kinase may play a role in regulating Scd1 diffusion. Indeed, the half-life of fluorescence decay in *pak1-ts* mutants is even slower than that of Scd1-3xGFP. This further highlights how Scd1 diffusion is dependent on its intrinsic properties and not just on its mass.

Scd1 is recruited to the cell membrane in its dephosphorylated form (Das et al., 2012). Given that our data show that Scd1 diffuses from one end of the cell to the next, it raises the possibility that a phosphatase is involved in this regulation where it dephosphorylates Scd1, thereby enabling membrane recruitment and Cdc42 activation. Such a kinase-phosphatase based regulatory system along with diffusion in the cytoplasm can allow the periodic redistribution of Scd1 at the cell ends to promote bipolar growth. Further investigations will define if similar diffusion dependent localization of Cdc42 GEFs also occur in animal cells to enable multipolar growth.

While the role for protein diffusion in the cytoplasm has not been clearly understood in biological systems, a recent report has shown that increasing cytoplasmic viscosity impairs protein diffusion in the cell and this can impact dynamic cellular processes (Molines et al., 2022). Cytoplasmic viscosity has impacts protein diffusion in both fission yeast cells as well as in animal cells. Thus, this may be a conserved form of regulation and further studies will define the mechanistic details of diffusion of Scd1 and other proteins in polarity control.

MATERIALS AND METHODS

Strains and Cell Culture

The *S. pombe* strains used in this study are listed in Table S1. All strains are isogenic to the original strain PN567. Cells were cultured in yeast extract (YE) medium and grown exponentially at 25°C unless specified otherwise. Standard techniques were used for genetic manipulation and analysis (Moreno et al., 1991). Cells were grown exponentially for at least three rounds of eight generations each before imaging.

Microscopy

Imaging was performed at room temperature (23–25°C). We used a Nikon Ti2 Eclipse wide-field microscope with a 100×/1.49 NA objective and an ORCA-FusionBT digital camera (Hamamatsu Model: C15440-20UP Serial No: 500428). Images were acquired using Nikon NIS Elements (Nikon). Fluorophores were excited with an AURA Light Engine system (Lumencor).

Microscopy was also performed with a 3i spinning disk confocal using a Zeiss AxioObserver microscope with an integrated Yokogawa spinning disk (Yokogawa CSU-X1 A1 spinning disk scanner) and a 100×/1.49 NA objective. Images were acquired with a Teledyne Photometrics Prime 95b back illuminated sCMOS camera (Serial No: A20D203014). Images were acquired using SlideBook (3i Intelligent Imaging innovations).

Acquiring and Quantifying Fluorescence Intensity

Fluorescence intensity was measured using ImageJ software. All images were sum projected and mean intensities were reported. Freehand ROIs were used to measure the signal at the cell ends. For analysis of two ends of the same cell, cytoplasm with little or no signal was

302 used for background subtraction. For all other experiments, a region outside of the cell was
303 used for background subtraction. The mean intensity was measured and recorded after the
304 background subtractions.

305 For FLIP analysis, cells were imaged every 10 s for 10 minutes with 4% laser power at
306 488nm wavelength. Bleaching repeatedly occurs every 2nd timepoint (1 bleach every 20
307 seconds). The resulting FLIP data was fitted to a one-phase decay curve to indicate the time to
308 lose 50% of fluorescence at the opposite cell end for each cell in each experiment.

309 For FRAP analysis, cells were imaged every 250 ms for 30 s with 15% laser power at
310 488nm wavelength. Square 10 x 10 Pixel (1.1 × 1.1 μm) ROIs were used to target, bleach, and
311 measure the fluorescence intensity at half of one cell end as it was bleached and then allowed
312 to recover. The first nine time points were acquired before photobleaching and served as a
313 measurement of the initial fluorescence intensity. On the 10th time point, the acquisition was
314 halted momentarily and the region of interest was photobleached using three 4% laser power
315 bleach repetitions with a duration of 5 ms each (15 ms total). After the region of interest was
316 bleached, acquisition resumed at 250 ms intervals as the fluorescence intensity recovered. The
317 half-life of fluorescence recovery was quantified using SlideBook FRAP analysis software.

318 To quantify signal stability at the cell ends, cells were imaged every 30 s for 20 min. The
319 stability of the proteins was then quantified by measuring the difference in intensity between
320 each subsequent time point for the duration of the timelapse imaging. Populations that had
321 larger average variations of fluorescent intensity between each timepoint were more dynamic
322 and less stable than populations that had smaller variations between each timepoint.

323

324 **Statistical tests**

Significance was determined using GraphPad Prism. When comparing two conditions, a Student's t-test was used (two-tailed, unequal variance). One-way ANOVA, followed by Tukey's multiple comparison tests, was used to determine significance of experiments with three or more conditions. SuperPlots (Lord et al., 2020) were made using GraphPad Prism.

330 **FIGURE LEGENDS**

331 **Figure 1. Scd1 is highly cytoplasmic and diffuses along the cytoplasm between cell ends.**
332 (A) Scd1-mNG localization in *for3*$^{+}$ cells compared to *for3*Δ mutants. Magenta rectangle indicates
333 the cell example shown in C. (B) Quantification of mean Scd1-mNG intensity at cell ends in the
334 indicated strains. (C) Averaged plot profile of end-to-end Scd1-mNG distribution along the long
335 axis of the cell in G2 cells (n=59). (D) The ratio of cytoplasmic intensity relative to intensity at the
336 cell ends (N=3, n=59). (E) Diagram illustrating fluorescence loss in photobleaching (FLIP). Top:
337 If there is exchange of protein between the cytoplasm and the opposite cell end, we will see loss
338 in fluorescence at the end. The fluorescence decay graphs will determine the rate of diffusion.
339 Bottom: If there is no exchange of protein between the two halves of the cell, we will not see loss
340 of fluorescence at the opposite cell end. (F) FLIP performed on Scd1-mNG expressing cell.
341 Magenta dotted outline indicates the bleached cell. Cyan asterisk shows the repeatedly bleached
342 region. Magenta arrow indicates when about 50% of the fluorescence is lost at the cell end. Blue
343 arrow indicates roughly when all signal is lost at the cell end. (G) FLIP experiments are pooled
344 and fitted to a one phase decay curve. (H) Quantification of the time to lose 50% of fluorescence
345 (half-life) of Scd1-mNG in FLIP experiments. Scale bar, 10 μm. n.s., not significant; P value,
346 *<0.05 , Student's t test.

347

348 **Figure 2. Dampened Scd1 dynamics correlate with dampened Cdc42 activation. (A)**
349 Montage of CRIB-mCherry dynamics in Scd1-mNG cells and Scd1-3xGFP cells. **(B)**
350 Representative graphs of CRIB-mCherry dynamics in Scd1-mNG cells and Scd1-3xGFP cells.
351 **(C)** Quantification of the extent of Pak1-mEGFP fluctuations at the cell ends (N = 3, n ≥ 5 cells).
352 (**D)** Quantification of the percentage of monopolar cells observed in each culture. (N=3, n ≥ 10
353 cells). Scale bar, 10 μm. P value, *<0.05, **<0.005, ****<0.0001, Student's t test and one-way
354 ANOVA followed by Tukey's multiple comparison test.

355

356 **Figure 3. FLIP and FRAP analysis of Scd1 with additional mass. (A)** Scd1-mNG, -2xGFP,
357 and -3xGFP cells were subjected to FLIP and loss in fluorescence was pooled and fitted to a
358 one-phase decay curve (n≥15). **(B)** Comparison of the half-lives of fluorescence loss in Scd1-
359 mNG, -2xGFP, and -3xGFP cells (n≥15). **(C)** FRAP will be used to completely bleach half of one
360 cell end and we will quantify the rate of fluorescence recovery at this cell end. (**D)** Averaged
361 FRAP graphs for Scd1-mNG, -2xGFP and -3xGFP. (n≥13). **(E)** Quantification of the half-lives of
362 FRAP in cells expressing Scd1-mNG, -2xGFP, and -3xGFP. (n≥17). Scale bar, 10 µm. n.s., not
363 significant; P value, *<0.05, **<0.005, one-way ANOVA followed by Tukey's multiple comparison
364 test.
365
366 **Figure 4. Loss of *pak1* kinase decreases Scd1 diffusion rates. (**A) Montage of Scd1-mNG
367 FRAP in *pak1*$^{+}$ and *pak1-ts* cells. Magenta boxes indicate the half of the cell end that has been
368 photobleached. Magenta arrows show when half of the final fluorescence has recovered. Blue
369 arrows indicate when the fluorescence recovery plateaus. (B) Averaged fluorescence recovery
370 graphs of Scd1-mNG FRAP in *pak1*$^{+}$ and *pak1-ts* cells. (C) Half-life of fluorescence recovery in
371 *pak1*$^{+}$ and *pak1-ts* cells (n≥16). (D) FLIP of Scd1-mNG in *pak1*$^{+}$ and *pak1-ts* cells cells. The
372 fluorescence loss at the cell ends was pooled and fitted to a one-phase decay (n≥10). (E)
373 Quantification of Scd1-mNG loss at the cell ends of *pak1*$^{+}$ and *pak1-ts* cells (n≥10). Scale bar,
374 10 µm. n.s., not significant; P value, *<0.05, Student's t test.
375
376 **Figure 5. FLIP reveals that Scd1 diffuses between the cytoplasm and cell ends more**
377 **rapidly than Scd2.** (A) Cellular localization of Scd1-mNG and Scd2-GFP. (B) End-to-end
378 fluorescence intensity profiles of Scd1-mNG and Scd2-GFP along the long axis of the cell (n=
379 60). (C) Ratio of cytoplasmic intensity relative to the intensity at the cell ends for Scd1-mNG
380 compared to Scd2-GFP (N=3, n = 20 cells per replicate). (D) Montages of FLIP in Scd1-mNG
381 and Scd2-GFP. Magenta dotted line indicates the bleached cell. Cyan asterisk shows the

382 repeatedly bleached region. Magenta arrow indicates roughly when 50% of fluorescence is lost
383 at the cell end. Blue arrow indicates roughly when all signal is lost at the cell end. (E) Pooled
384 fluorescence loss for Scd1-mNG and Scd2-GFP fitted to a one phase decay curve (n ≥16). (F)
385 Half-lives of fluorescence loss in Scd1-mNG compared to Scd2-GFP (n ≥16). (H) One phase
386 decay curve of fluorescence loss of Scd2-GFP data repurposed from Figure 4 and Scd1-2xGFP
387 and -3xGFP data repurposed from Figure 2 (n≥15). Scale bar, 10 μm. n.s., not significant; P
388 value, **<0.005, ***<0.0009, Student's t test.

REFERENCES

Axelrod, D., Koppel, D. E., Schlessinger, J., Elson, E. and Webb, W. W. (1976). Mobility measurement by analysis of fluorescence photobleaching recovery kinetics. *Biophys J* **16**, 1055-69.

Butty, A. C. (2002). A positive feedback loop stabilizes the guanine-nucleotide exchange factor Cdc24 at sites of polarization. *The EMBO Journal* **21**, 1565-1576.

Butty, A. C., Perrinjaquet, N., Petit, A., Jaquenoud, M., Segall, J. E., Hofmann, K., Zwahlen, C. and Peter, M. (2002). A positive feedback loop stabilizes the guanine-nucleotide exchange factor Cdc24 at sites of polarization. *Embo j* **21**, 1565-76.

Chang, E., Bartholomeusz, G., Pimental, R., Chen, J., Lai, H., Wang, L.-H. L., Yang, P. and Marcus, S. (1999). Direct Binding and In Vivo Regulation of the Fission Yeast p21-Activated Kinase Shk1 by the SH3 Domain Protein Scd2. *Molecular and Cellular Biology* **19**, 8066-8074.

Chang, E. C., Barr, M., Wang, Y., Jung, V., Xu, H. P. and Wigler, M. H. (1994). Cooperative interaction of S. pombe proteins required for mating and morphogenesis. *Cell* **79**, 131-41.

Cole, N. B., Smith, C. L., Sciaky, N., Terasaki, M., Edidin, M. and Lippincott-Schwartz, J. (1996). Diffusional mobility of Golgi proteins in membranes of living cells. *Science* **273**, 797-801.

Coll, P. M., Trillo, Y., Ametzazurra, A. and Perez, P. (2003). Gef1p, a new guanine nucleotide exchange factor for Cdc42p, regulates polarity in Schizosaccharomyces pombe. *Mol Biol Cell* **14**, 313-23.

Das, M., Drake, T., Wiley, D. J., Buchwald, P., Vavylonis, D. and Verde, F. (2012). Oscillatory Dynamics of Cdc42 GTPase in the Control of Polarized Growth. *Science* **337**, 239-243.

Das, M. and Verde, F. (2013). Role of Cdc42 dynamics in the control of fission yeast cell polarization. *Biochem Soc Trans* **41**, 1745-9.

Feierbach, B. and Chang, F. (2001). Roles of the fission yeast formin for3p in cell polarity, actin cable formation and symmetric cell division. *Curr Biol* **11**, 1656-65.

Gulli, M. P., Jaquenoud, M., Shimada, Y., Niederhäuser, G., Wiget, P. and Peter, M. (2000). Phosphorylation of the Cdc42 exchange factor Cdc24 by the PAK-like kinase Cla4 may regulate polarized growth in yeast. *Mol Cell* **6**, 1155-67.

Hall, A. (1990). The cellular functions of small GTP-binding proteins. *Science* **249**, 635-40.

Harrell, M. A., Liu, Z., Campbell, B. F., Chinsen, O., Hong, T. and Das, M. (2024). Arp2/3-dependent endocytosis ensures Cdc42 oscillations by removing Pak1-mediated negative feedback. *J Cell Biol* **223**.

Hercyk, B. S., Rich-Robinson, J., Mitoubsi, A. S., Harrell, M. A. and Das, M. E. (2019). A novel interplay between GEFs orchestrates Cdc42 activity during cell polarity and cytokinesis. *Journal of Cell Science* **132**, jcs236018.

Howell, A. S., Jin, M., Wu, C. F., Zyla, T. R., Elston, T. C. and Lew, D. J. (2012). Negative feedback enhances robustness in the yeast polarity establishment circuit. *Cell* **149**, 322-33.

Jacobson, K., Derzko, Z., Wu, E.-S., Hou, Y. and Poste, G. (1976). Measurement of the lateral mobility of cell surface components in single living cells by fluorescence recovery after photobleaching. *Journal of Supramolecular Structure* **5**, 565-576.

Johnson, D. I. (1999). Cdc42: An essential Rho-type GTPase controlling eukaryotic cell polarity. *Microbiol Mol Biol Rev* **63**, 54-105.

Kozubowski, L., Saito, K., Johnson, J. M., Howell, A. S., Zyla, T. R. and Lew, D. J. (2008). Symmetry-Breaking Polarization Driven by a Cdc42p GEF-PAK Complex. *Current Biology* **18**, 1719-1726.

Kuo, C. C., Savage, N. S., Chen, H., Wu, C. F., Zyla, T. R. and Lew, D. J. (2014). Inhibitory GEF phosphorylation provides negative feedback in the yeast polarity circuit. *Curr Biol* **24**, 753-9.

Lord, S. J., Velle, K. B., Mullins, R. D. and Fritz-Laylin, L. K. (2020). SuperPlots: Communicating reproducibility and variability in cell biology. *J Cell Biol* **219**.

Martin, S. G. and Chang, F. (2006). Dynamics of the formin for3p in actin cable assembly. *Curr Biol* **16**, 1161-70.

Matsuyama, A., Arai, R., Yashiroda, Y., Shirai, A., Kamata, A., Sekido, S., Kobayashi, Y., Hashimoto, A., Hamamoto, M., Hiraoka, Y. et al. (2006). ORFeome cloning and global analysis of protein localization in the fission yeast Schizosaccharomyces pombe. *Nature Biotechnology* **24**, 841-847.

Miller, P. J. and Johnson, D. I. (1994). Cdc42p GTPase Is Involved in Controlling Polarized Cell Growth in Schizosaccharomyces pombe. *Molecular and Cellular Biology* **14**, 1075-1083.

Molines, A. T., Lemiere, J., Gazzola, M., Steinmark, I. E., Edrington, C. H., Hsu, C. T., Real-Calderon, P., Suhling, K., Goshima, G., Holt, L. J. et al. (2022). Physical properties of the cytoplasm modulate the rates of microtubule polymerization and depolymerization. *Dev Cell* **57**, 466-479 e6.

Moreno, S., Klar, A. and Nurse, P. (1991). Molecular genetic analysis of fission yeast Schizosaccharomyces pombe. *Methods Enzymol* **194**, 795-823.

Murray, J. M. and Johnson, D. I. (2001). The Cdc42p GTPase and Its Regulators Nrf1p and Scd1p Are Involved in Endocytic Trafficking in the Fission YeastSchizosaccharomyces pombe *. *Journal of Biological Chemistry* **276**, 3004-3009.

Nakano, K., Imai, J., Arai, R., Toh, E. A., Matsui, Y. and Mabuchi, I. (2002). The small GTPase Rho3 and the diaphanous/formin For3 function in polarized cell growth in fission yeast. *J Cell Sci* **115**, 4629-39.

Nobes, C. D. and Hall, A. (1999). Rho GTPases control polarity, protrusion, and adhesion during cell movement. *J Cell Biol* **144**, 1235-44.

Poo, M. and Cone, R. A. (1974). Lateral diffusion of rhodopsin in the photoreceptor membrane. *Nature* **247**, 438-41.

Rapali, P., Mitteau, R., Braun, C., Massoni-Laporte, A., Ünlü, C., Bataille, L., Arramon, F. S., Gygi, S. P. and McCusker, D. (2017). Scaffold-mediated gating of Cdc42 signalling flux. *Elife* **6**.

Rossman, K. L., Der, C. J. and Sondek, J. (2005). GEF means go: turning on RHO GTPases with guanine nucleotide-exchange factors. *Nature Reviews Molecular Cell Biology* **6**, 167-180.

Sawin, K. E. and Nurse, P. (1998). Regulation of cell polarity by microtubules in fission yeast. *J Cell Biol* **142**, 457-71.

Scheffzek, K. and Ahmadian, M. R. (2005). GTPase activating proteins: structural and functional insights 18 years after discovery. *Cellular and Molecular Life Sciences CMLS* **62**, 3014-3038.

Shcheprova, Z., Baldi, S., Frei, S. B., Gonnet, G. and Barral, Y. (2008). A mechanism for asymmetric segregation of age during yeast budding. *Nature* **454**, 728-734.

Stengel, K. and Zheng, Y. (2011). Cdc42 in oncogenic transformation, invasion, and tumorigenesis. *Cellular Signalling* **23**, 1415-1423.

Verde, F., Wiley, D. J. and Nurse, P. (1998). Fission yeast orb6, a ser/thr protein kinase related to mammalian rho kinase and myotonic dystrophy kinase, is required for maintenance of

487 cell polarity and coordinates cell morphogenesis with the cell cycle. *Proc Natl Acad Sci U S A*
488 **95**, 7526-31.
489 **Verkman, A. S.** (2002). Solute and macromolecule diffusion in cellular aqueous
490 compartments. *Trends in Biochemical Sciences* **27**, 27-33.
491 **Wei, B., Hercyk, B. S., Mattson, N., Mohammadi, A., Rich, J., DeBruyne, E., Clark,**
492 **M. M. and Das, M.** (2016). Unique spatiotemporal activation pattern of Cdc42 by Gef1 and Scd1
493 promotes different events during cytokinesis. *Mol Biol Cell* **27**, 1235-45.
494 **Wheatley, E. and Rittinger, K.** (2005). Interactions between Cdc42 and the scaffold
495 protein Scd2: requirement of SH3 domains for GTPase binding. *Biochem J* **388**, 177-84.
496 **White, J. and Stelzer, E.** (1999). Photobleaching GFP reveals protein dynamics inside
497 live cells. *Trends in Cell Biology* **9**, 61-65.
498 **Wu, C. F., Chiou, J. G., Minakova, M., Woods, B., Tsygankov, D., Zyla, T. R., Savage,**
499 **N. S., Elston, T. C. and Lew, D. J.** (2015). Role of competition between polarity sites in
500 establishing a unique front. *Elife* **4**.
501 **Wu, C. F. and Lew, D. J.** (2013). Beyond symmetry-breaking: competition and negative
502 feedback in GTPase regulation. *Trends Cell Biol* **23**, 476-83.
503 **Zhang, B., Zhang, Y., Collins, C. C., Johnson, D. I. and Zheng, Y.** (1999). A built-in
504 arginine finger triggers the self-stimulatory GTPase-activating activity of rho family GTPases. *J*
505 *Biol Chem* **274**, 2609-12.

506

Figure 1

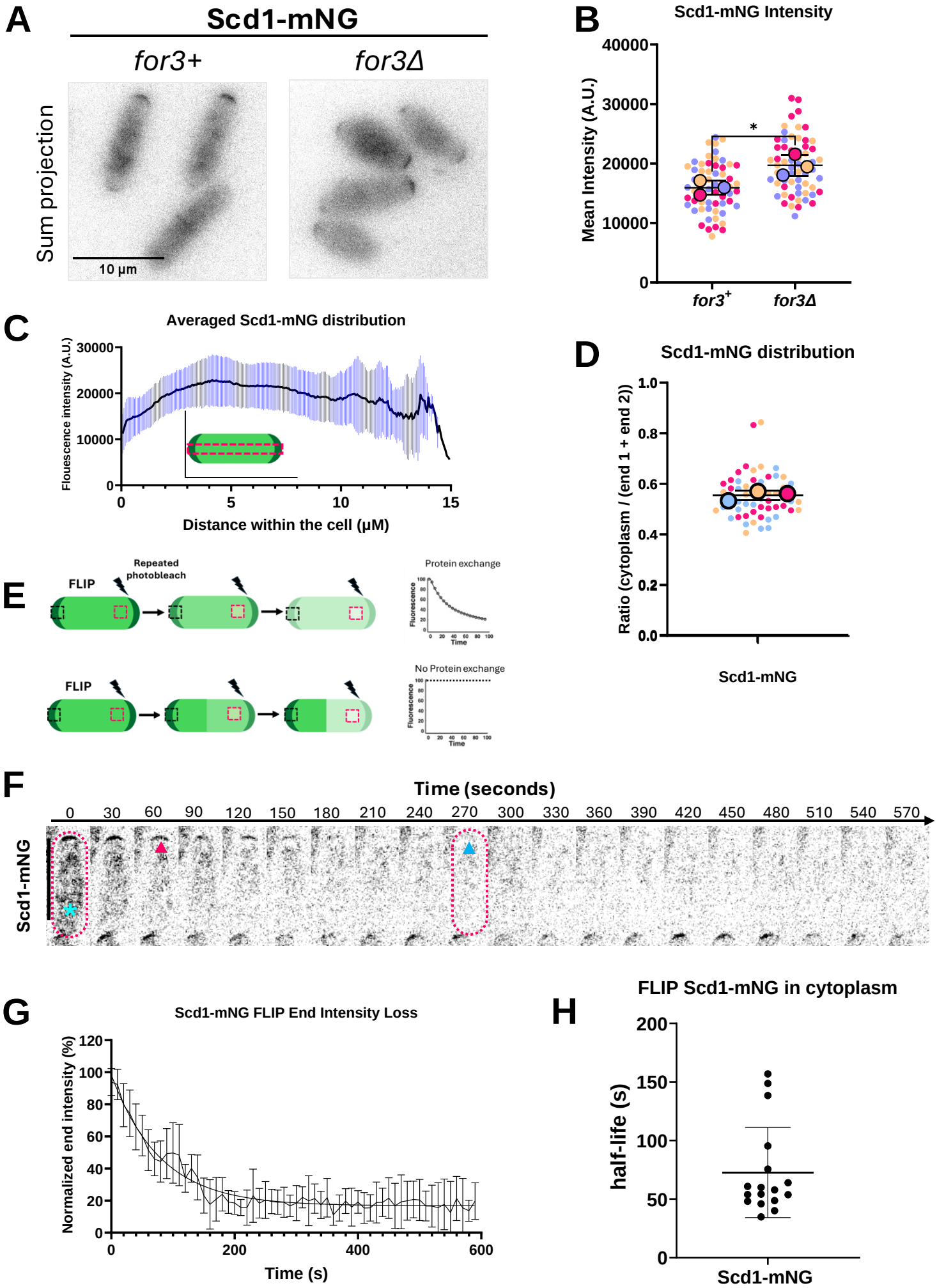
A
Scd1-mNG
for3+
for3Δ
Sum projection
10 µm
B
Scd1-mNG Intensity
Mean Intensity (A.U.)
40000
30000
20000
10000
0
*
for3+
for3Δ
C
Averaged Scd1-mNG distribution
Flouescence intensity (A.U.)
30000
20000
10000
0
0
5
10
15
Distance within the cell (µM)
D
Scd1-mNG distribution
Ratio (cytoplasm / (end 1 + end 2))
1.0
0.8
0.6
0.4
0.2
0.0
Scd1-mNG
E
FLIP
Repeated photobleach
Protein exchange
Fluorescence
Time
FLIP
No Protein exchange
Fluorescence
Time
F
Time (seconds)
0 30 60 90 120 150 180 210 240 270 300 330 360 390 420 450 480 510 540 570
Scd1-mNG
G
Scd1-mNG FLIP End Intensity Loss
Normalized end intensity (%)
120
100
80
60
40
20
0
0
200
400
600
Time (s)
H
FLIP Scd1-mNG in cytoplasm
half-life (s)
200
150
100
50
0
Scd1-mNG

Figure 2

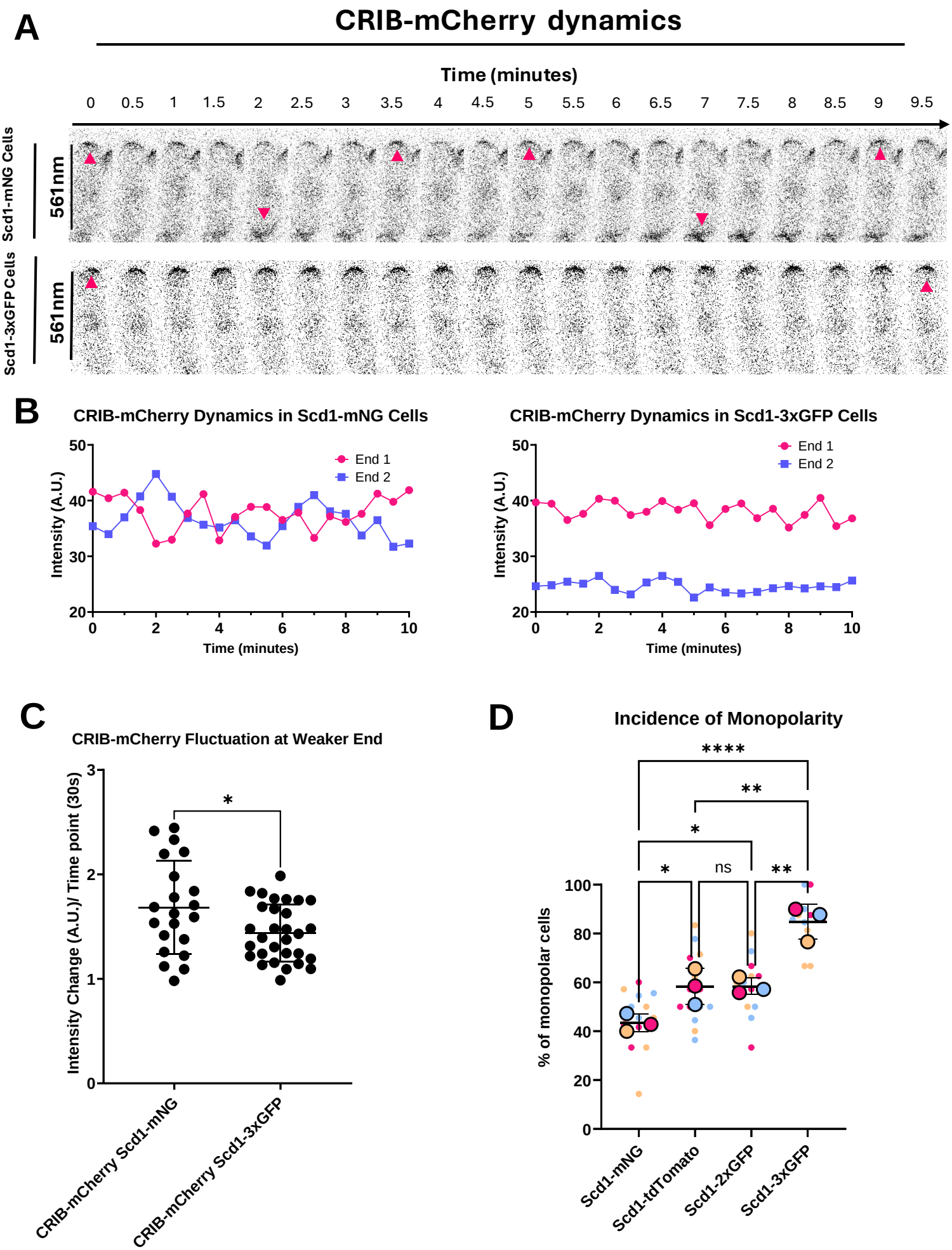
A
CRIB-mCherry dynamics
Time (minutes)
0 0.5 1 1.5 2 2.5 3 3.5 4 4.5 5 5.5 6 6.5 7 7.5 8 8.5 9 9.5
Scd1-mNG Cells
561 nm
Scd1-3xGFP Cells
561 nm
B
CRIB-mCherry Dynamics in Scd1-mNG Cells
CRIB-mCherry Dynamics in Scd1-3xGFP Cells
End 1
End 2
Intensity (A.U.)
Time (minutes)
C
CRIB-mCherry Fluctuation at Weaker End
Intensity Change (A.U.)/ Time point (30s)
*
CRIB-mCherry Scd1-mNG
CRIB-mCherry Scd1-3xGFP
D
Incidence of Monopolarity
% of monopolar cells
****
**
*
ns
Scd1-mNG
Scd1-tdTomato
Scd1-2xGFP
Scd1-3xGFP

Figure 3

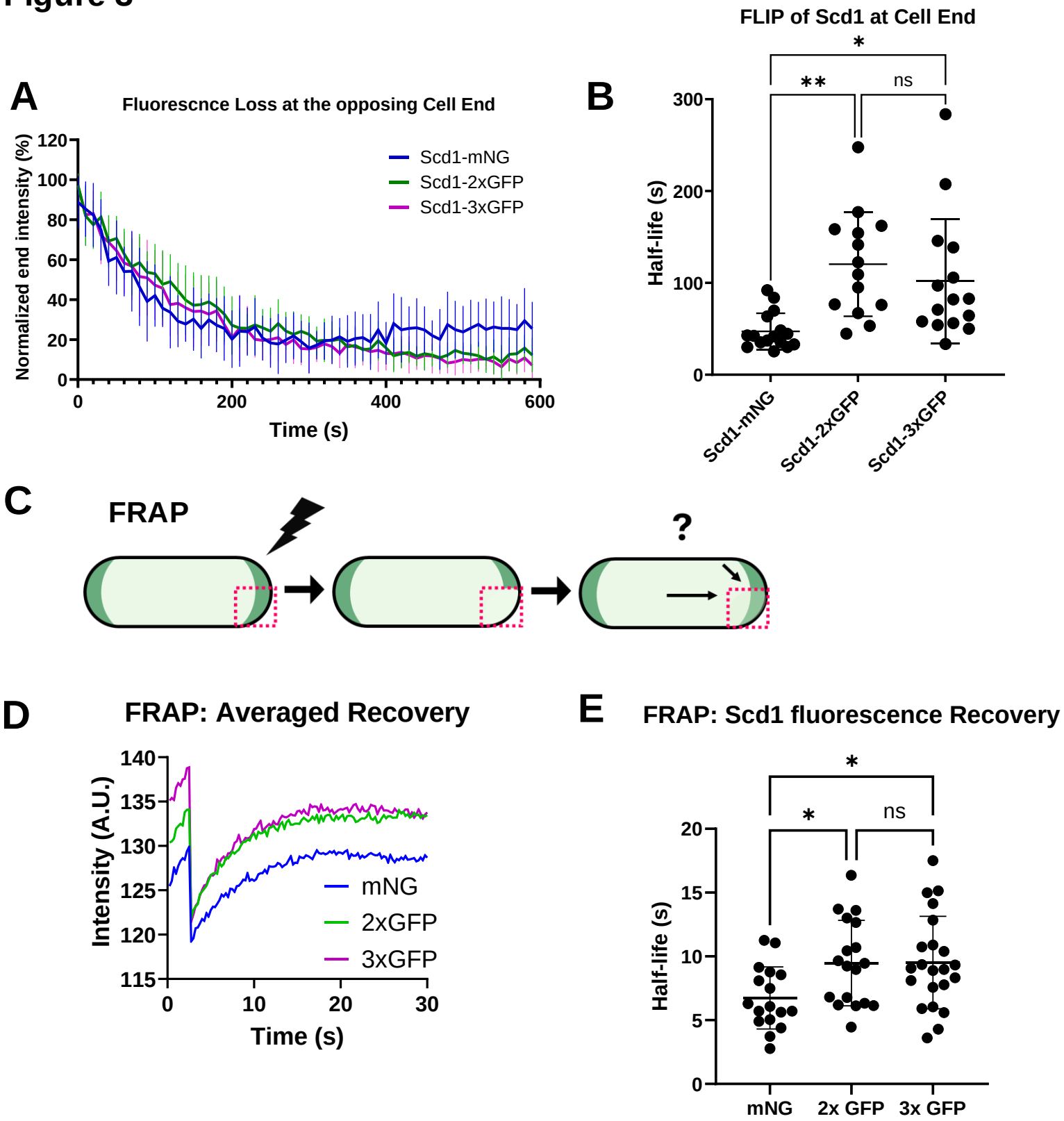
A
Fluorescnce Loss at the opposing Cell End
Normalized end intensity (%)
Time (s)
Scd1-mNG
Scd1-2xGFP
Scd1-3xGFP
B
FLIP of Scd1 at Cell End
Half-life (s)
*
**
ns
Scd1-mNG
Scd1-2xGFP
Scd1-3xGFP
C
FRAP
?
D
FRAP: Averaged Recovery
Intensity (A.U.)
Time (s)
mNG
2xGFP
3xGFP
E
FRAP: Scd1 fluorescence Recovery
Half-life (s)
*
*
ns
mNG
2x GFP
3x GFP

Figure 4

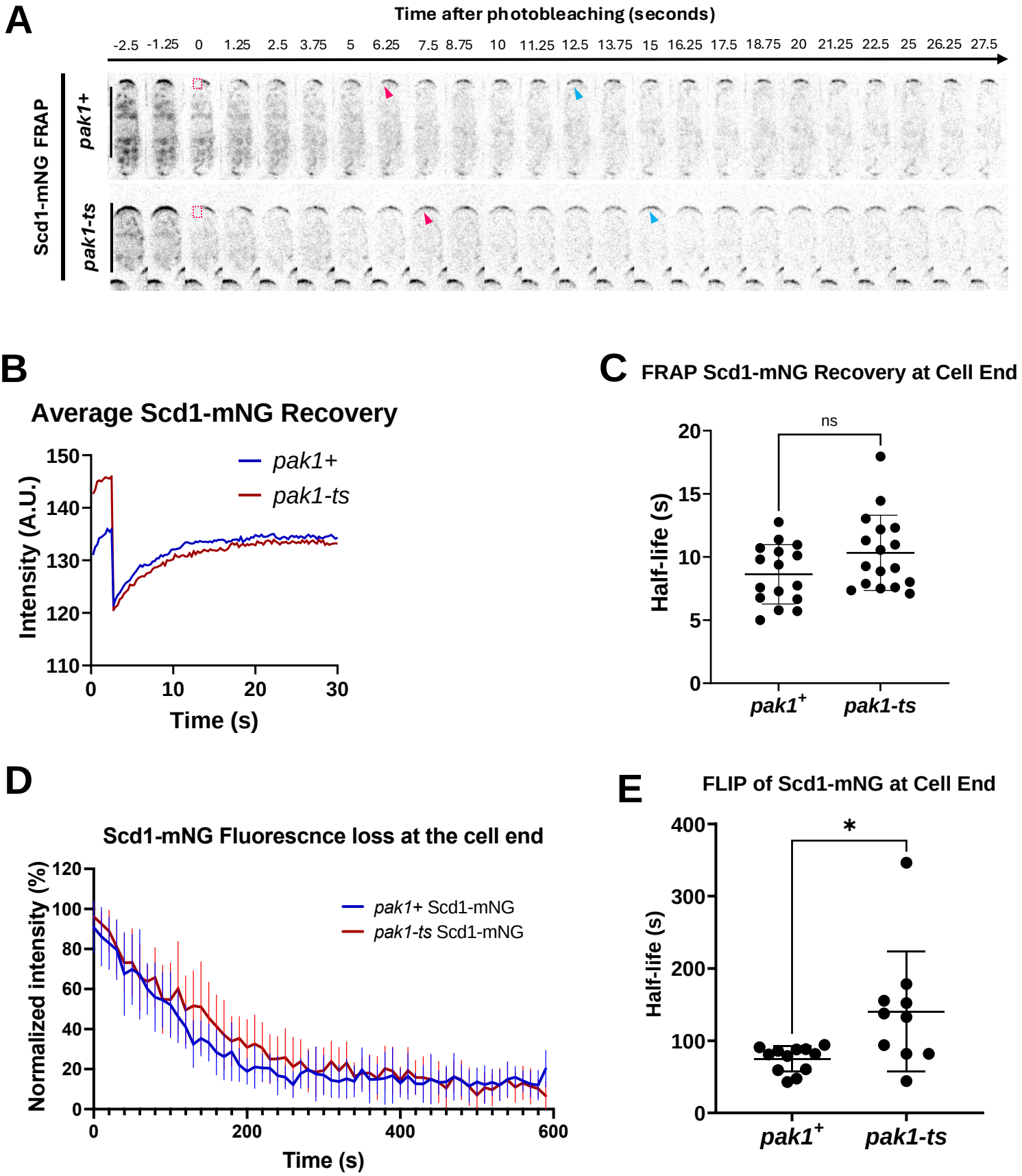
A
Time after photobleaching (seconds)
-2.5 -1.25 0 1.25 2.5 3.75 5 6.25 7.5 8.75 10 11.25 12.5 13.75 15 16.25 17.5 18.75 20 21.25 22.5 25 26.25 27.5
Scd1-mNG FRAP
pak1+
pak1-ts
B
Average Scd1-mNG Recovery
Intensity (A.U.)
150
140
130
120
110
0
10
20
30
Time (s)
pak1+
pak1-ts
C
FRAP Scd1-mNG Recovery at Cell End
ns
Half-life (s)
20
15
10
5
0
pak1+
pak1-ts
D
Scd1-mNG Fluorescnce loss at the cell end
Normalized intensity (%)
120
100
80
60
40
20
0
0
200
400
600
Time (s)
pak1+ Scd1-mNG
pak1-ts Scd1-mNG
E
FLIP of Scd1-mNG at Cell End
*
Half-life (s)
400
300
200
100
0
pak1+
pak1-ts

Figure 5

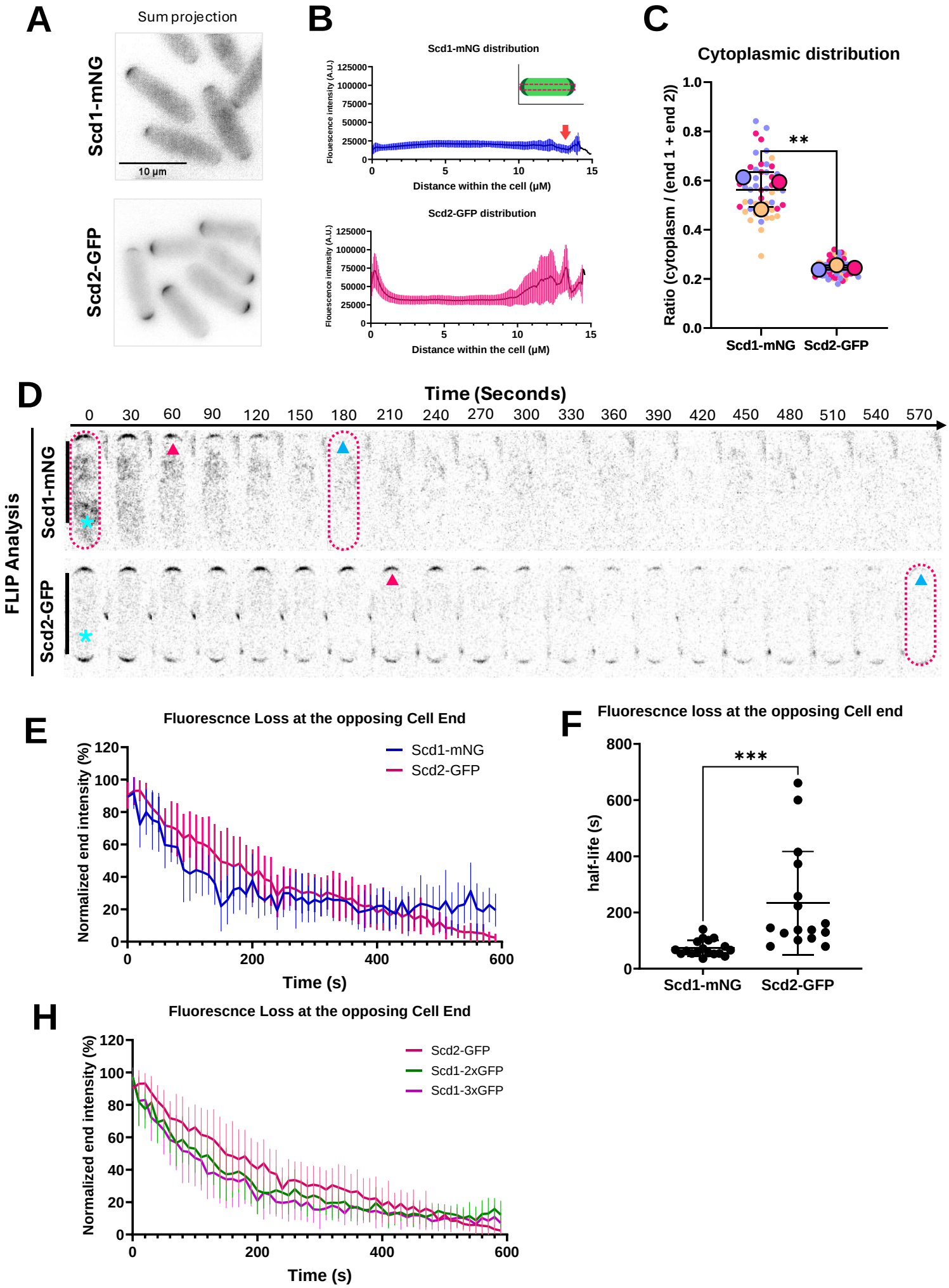
A
Sum projection
Scd1-mNG
Scd2-GFP
10 µm
B
Scd1-mNG distribution
Flouescence intensity (A.U.)
Distance within the cell (µM)
Scd2-GFP distribution
C
Cytoplasmic distribution
Ratio (cytoplasm / (end 1 + end 2))
**
Scd1-mNG
Scd2-GFP
D
Time (Seconds)
FLIP Analysis
Scd1-mNG
Scd2-GFP
E
Fluorescnce Loss at the opposing Cell End
Normalized end intensity (%)
Time (s)
Scd1-mNG
Scd2-GFP
F
Fluorescnce loss at the opposing Cell end
half-life (s)
***
Scd1-mNG
Scd2-GFP
H
Fluorescnce Loss at the opposing Cell End
Normalized end intensity (%)
Time (s)
Scd2-GFP
Scd1-2xGFP
Scd1-3xGFP